HHS Public Access

Author manuscript

Acta Biomater. Author manuscript; available in PMC 2023 January 15.

Published in final edited form as:

Acta Biomater. 2022 January 15; 138: 351–360. doi:10.1016/j.actbio.2021.10.051.

The Stoic Tooth Root: How the Mineral and Extracellular Matrix Counterbalance to Keep Aged Dentin Stable

Mariana Reis[a,b], **Yvette Alania**[a,b], **Ariene Leme-Kraus**[b], **Robert Free**[c], **Derk Joester**[c], **Weikang Ma**[d], **Thomas Irving**[d], **Ana K. Bedran-Russo**[a,b]

[a]Department of General Dental Sciences, Marquette University, Milwaukee, WI, USA

[b]Department of Restorative Dentistry, University of Illinois at Chicago, Chicago, IL, USA

[c]Department of Materials Science and Engineering, Northwestern University, Evanston, IL, USA

[d]Department of Biological Sciences, Illinois Institute of Technology. Chicago, IL, USA

Abstract

Aging is a physiological process with profound impact on the biology and function of biosystems, including the human dentition. While resilient, human teeth undergo wear and disease, affecting overall physical, psychological, and social human health. However, the underlying mechanisms of tooth aging remain largely unknown. Root dentin is integral to tooth function in that it anchors and dissipates mechanical load stresses of the tooth-bone system. Here, we assess the viscoelastic behavior, composition, and ultrastructure of young and old root dentin using nano-dynamic mechanical analysis, micro-Raman spectroscopy, small angle X-ray scattering, atomic force and transmission electron microscopies. We find that the root dentin overall stiffness increases with age. Unlike other mineralized tissues and even coronal dentin, the ability of root dentin to dissipate energy during deformation does not decay with age. Using a deconstruction method to dissect the contribution of mineral and organic matrix, we find that the damping factor of the organic matrix does deteriorate. Compositional and ultrastructural analyses revealed higher mineral-to-matrix ratio, altered enzymatic and non-enzymatic collagen cross-linking, increased collagen *d*-spacing and fibril diameter, and decreased abundance of proteoglycans and sulfation pattern of glycosaminoglycans. Therefore, even in the absence of remodeling, the extracellular matrix of root dentin shares traits of aging with other tissues. To explain this discrepancy, we propose that altered matrix-mineral interactions, possibly mediated by carbonate ions sequestered at the mineral interface and/or altered glycosaminoglycans counteract the deleterious effects of aging on the structural components of the extracellular matrix.

Corresponding Author Ana K. Bedran-Russo, Department of General Dental Sciences, Marquette University, 1801, West Wisconsin Ave, room 336C, Milwaukee, WI, 53233 USA Phone number: (414) 288 5409. ana.bedran-russo@marquette.edu.

Declaration of interests

The authors declare that they have no known competing financial interests or personal relationships that could have appeared to influence the work reported in this paper.

Statement of significance: Globally, a quarter of the population will be over 65 years old by 2050. Because many will retain their dentition, it will become increasingly important to understand and manage how aging affects teeth. Dentin is integral to the protective, biomechanical, and regenerative features of teeth. Here, we demonstrate that older root dentin not only has altered mechanical properties, but shows characteristic shifts in mineralization, composition, and post-translational modifications of the matrix. This strongly suggests that there is a mechanistic link between mineral and matrix components to the biomechanical performance of aging dentin with implications for efforts to slow or even reverse the aging process.

Graphical Abstract

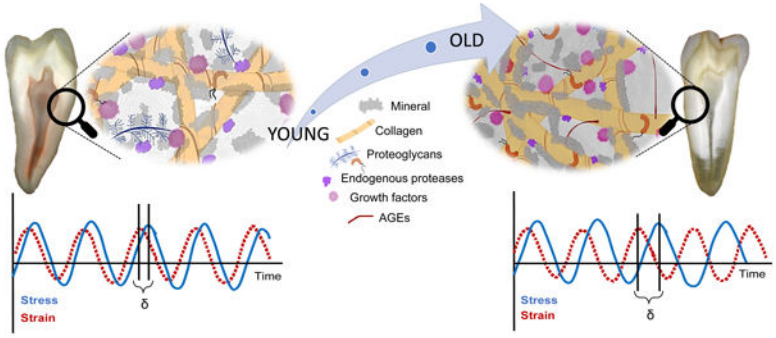

Keywords

Aging; Dentin; Collagen; Viscoelastic behavior; Extracellular matrix

1. Introduction

Aging is the accumulation of physicochemical changes of tissues and organs over time and is associated with increasing susceptibility to disease and mortality [1,2]. Of particular importance is the progressive alteration of biomacromolecular components of the extracellular matrix (ECM). The direct impact of aging on the functional features of the ECM is magnified by the disruption of cell-matrix interactions and the resulting misregulation of cellular function [3]. The aging of mineralized tissues such as bone and teeth is further dependent on the ECM-biomineral interactions, affecting structure, composition, and biomechanics.

Bone undergoes continuous turnover and remodeling through enzymatic and non-enzymatic processes [4,5] and, with age, these processes are known to alter the ECM composition [6]. For instance, bone exhibits shifts in length, crystallinity and mineral substitutions in the hydroxyapatite lattice [7,8], ratio of post-translational modification of collagen [9–11], accumulation of advanced glycation end-products (AGEs) [12–14], decrease in proteoglycan content and glycosaminoglycan sulfation patterns [10,15]. These compositional changes increase bone stiffness, resulting in reduced viscoelasticity and overall mechanical performance [16]. Interestingly, similar age-related modification of the ECM and reduced viscoelasticity are found in non-mineralized tissues such as skin, muscle and eyes [17–21].

In contrast to bone, teeth have essentially no turnover. The remarkable endurance of teeth is attributed to the composition and complex multi-scale structural arrangement, particularly of dentin. Dentin is a composite of nanocrystalline carbonate hydroxyapatite (~50 vol%), water (~20 %), and an ECM (~30%) largely composed of structural and regulatory components such as type I collagen, phosphoproteins, and proteoglycans (Fig. 1A). In addition to structural variations in tubule density and peritubular dentin thickness, crown and root dentin also differ in composition [22,23]. An important function of coronal dentin is to dissipate energy, thereby hindering propagation of cracks from the brittle enamel, and thus protect the vascular pulp tissue from injury. Root dentin, on the other hand, anchors the tooth to the alveolar bone and absorbs/dissipates stresses during mastication and resting states [24].

With aging, the mineral content of dentin increases [25], and biomechanical features degrade [26–30]. However, the underlying mechanisms of tooth aging remains largely unknown. Moreover, it is not clear to what degree age-related changes in dentin recapitulate those in bone and other organs that exhibit turnover, more specifically, the impact of post-translational modifications of collagen and proteoglycans, two major structural components of the dentin ECM. Using a range of analytical techniques to probe the biochemistry, ultrastructure, and mechanical properties of dentin, the aim of this study was to reveal age-related modifications of the dentin matrix and their contribution to the viscoelastic behavior of root dentin. The study hypothesis was that, similarly to bone, modifications to the mineral phase and the ECM incurred with age would negatively impact the viscoelastic behavior of root dentin, a key functional feature of teeth.

2. Materials and methods

2.1. Biospecimen preparation

Extracted human bicuspids were selected following institutional review board approval (2018–0346). The teeth roots of adults 18 – 25 years of age (young, n = 6) and 50 – 80 years of age (old, n = 6) were selected after careful evaluation of tooth biospecimens morphological traits and age groups were established based on previous studies [27,31,32]. Specimens were either bisected sagittally or cut into dentin sections of ~500 μm thickness (Fig 1B). Sections were randomly assigned to compositional, morphological, ultrastructural and nano-mechanical analyses (Fig 1B).

For Raman micro-spectroscopy, atomic force microscopy, and nano-mechanical analysis, bisected roots embedded in EpoxyCure 2 resin (Buehler) were ground with SiC paper (320 – 1200 grit) and polished with polycrystalline diamond suspensions (9 – 0.5 μm, Buehler). Dentin root slabs for small angle X-ray scattering and transmission electron microscopy analysis were ground with SiC paper (600 – 800 grit) to a final thickness of 100 μm.

The polished dentin surfaces were demineralized with 0.5 M EDTA for 1h (pH 8.0 at 4°C). Dentin root slabs were fully demineralized with 0.5 M EDTA for 72 h (pH 8.0 at 4°C) [33,34]. The removal of mineral content was assessed with X-ray analysis and samples were compared with fully mineralized samples (data not shown). Additionally, a subset of demineralized sections was depleted of proteoglycans by treatment with matrix metalloproteinase 3 (MMP-3, R&D Systems) at 1μg/mL in 100 mM Tris, 150 mM NaCl, 5

mM CaCl2, 0.05% Brij 35, and 0.02% NaN3 buffer (pH 7.2) for 48 h at 37°C) [35,36]. The cervical and apical root regions were studied (Fig. 1B).

2.2. Characterization of dentin by μ-Raman

Raman spectra were collected using inVia Raman microscope (Renishaw) in backscatter mode. The excitation wavelength was 633 nm and spectral range from 660 to 1780 cm^{-1} with a resolution of 4 cm^{-1}. Spectra were recorded in six distinct locations within each region (cervical and apical, n = 3). Each spectrum was recorded by accumulating 60 exposures, each with a 1 s exposure time. Spectra were baseline corrected using a cubic spline subtraction through chosen points on each spectrum and with optimized parameters (smoothed using 3rd order polynomial with a 19-point Savitzky-Golay algorithm) and then normalized with integrated signal to total intensity by a constant.

The analysis of Raman spectra enables the evaluation of a range of structural and compositional parameters in mineralized tissues [12,37–43]. Raman indices were obtained by area and or height of the assigned bands and calculated by peak fitting function in WiRE 4.3 (Renishaw, Gloucestershire, UK), Table S1. The carbonate substitution index is a measure of the extent of substitution of carbonate on phosphate lattice positions in apatite (type B). Also known as the mineral quality index (MQ-1), it is calculated as the ratio of the area of the type B carbonate $\nu1$ over that of the phosphate $\nu1$ band (A_{1070}/A_{958}). A higher value indicates a higher level of carbonate substitution. A second mineral quality index (MQ-2) is the reciprocal of the full width at half maximum of the phosphate $\nu1$ band ($1/FWHM_{958}$). A high degree of crystallinity is indicated by high values. Mineral phase was assessed using two mineral-to-matrix (MMR) indices. MMR-1 is the ratio of the area of the phosphate $\nu1$ over that of the amide I band (A_{958}/A_{1665}). MMR-2 is the ratio of the area of the phosphate $\nu1$ band over the wagging band of CH_2 (A_{958}/A_{1450}). High values of both indices indicate a high degree of mineralization.

Collagen post-translational modification (PTM), specifically enzymatic collagen cross-linking, and advanced glycation end-products (AGE) were assessed using two indices. PTM-1 indicates the ratio of non-reducible collagen cross-links to reducible ones and is calculated as A_{1656}/A_{1684}. PTM-2 is a measure of the abundance of AGEs and is calculated as the ratio of the intensity of a band at 1550 cm^{-1} over that of the CH_2 wagging mode (A_{1550}/A_{1450}).

Proteoglycan content and glycosaminoglycans chains (GAGs) sulfation pattern were evaluated using the PG-1, PG-2 and SPGAG indices. The PG-1 index is calculated as the ratio of the sum of the areas of bands representing chondroitin sulfate, aggrecan monomer and other PGs over the area of the amide I band ($A_{1065+1342+1370}/A_{1665}$). PG-2 is the ratio of the area of a band at 1370 cm^{-1} that is characteristic for PGs to the area of the CH_2 wagging mode (A_{1370}/A_{1450}). Higher values of PG-1 and PG-2 thus indicate that proteoglycans represent a larger fraction of the total protein present. SPGAG is calculated as the ratio of a band indicative of chondroitin-4-sulfate (C4S) at 730 cm^{-1} over the area of a band representative of PGs (A_{730}/A_{1370}). A higher value indicates that a higher fraction of chondroitin repeat units are sulfated in the 4-position.

2.3. Small angle x-ray scattering (SAXS)

SAXS patterns of mineralized, demineralized (dentin organic matrix) and PG-depleted dentin samples (n = 6) were collected at the BioCAT beamline 18ID, at Advanced Photon Source (Argonne National Laboratory). The incident beam energy was 12 keV, focused to a probe size of 20 μm x 4 μm, with an available flux density of 1×10^{12} photons s^{-1} mm^{-2}. MuscleX software [44] batch-fitting provided the following measurements for each pattern: average radial distance d of the 3rd order peak of the characteristic collagen *d*-spacing, maximum peak intensity (I), and azimuthal spread (orientational distribution: σ_θ). Assuming that the orientation distribution does not change significantly with age, the integrated intensity of the 3rd order reflection in SAXS patterns scales with the total amount of matter that exhibits the characteristic periodicity (*d*-spacing) of collagen (Fig. S1 and S2).

Specimens were sealed in Kapton® tape fully immersed in ultrapure water. The encased specimens were mounted on a translation stage, brought to the focal point of the beam, and SAXS patterns were collected in transmission. Root dentin was sampled in a series of line scans along the long axial direction (Fig. S2A). With a step size of 400 μm, each root section was sampled at 10–20 points in the axial and 4–10 points in the transverse direction, depending on the size. The exposure time per 2D-pattern was 500 ms. Data were processed with the FIT2D [45], Image J, and MuscleX software packages to calibrate raw datasets, perform background subtraction, and fit the 3rd order reflection of the characteristic ~67 nm collagen *d*-spacing. Inspection of the distribution of the collagen *d*-spacing did not reveal any trends with distance in the axial or transverse directions (Fig. S2B–C). Data were therefore averaged for the cervical and apical regions of the tooth. We assessed the characteristic periodicity (*d*-spacing) of collagen, the total diffracted intensity as a qualitative measure of the amount of diffracting material, and the distribution of collagen orientations.

2.4. Atomic force microscopy (AFM)

Demineralized dentin (the dentin organic matrix) and PG-depleted dentin were imaged (n = 3) in ultrapure water in a Dimension Icon atomic force microscope (Bruker) with ScanAsyst Fluid+ probes (nominal spring constant: 0.7 N/m and tip radius: 2–12 nm, Direct Drive Fluid Cell DTFML-DD). Imaging was performed at a scan rate of 1 Hz, scan size of 3 × 3 μm (~11.7 nm/pixel) at three different locations in each region (cervical and apical root). The diameter of individual collagen fibrils was extracted from line profiles taken across collagen fibrils over the width of a fibril identified in topographic maps. Diameters of eight fibrils per image were used to calculate the mean diameter (NanoScope Analysis 1.5).

2.5. Spatial distribution of PGs/GAGs

Spatial distribution and ultrastructure of GAGs in cervical root dentin were visualized in transmission electron microscope using previously described method [46]. Briefly, root dentin sections (n = 3) were fixed in formalin (1:10) for 4 days. Specimens were demineralized in 0.5 M EDTA (1.5 mL pH 8.0) at 4°C for 3 days and rinsed with ultrapure water. Specimens were then fixed in 2.5 vol% aqueous glutaraldehyde (1.5 mL, pH 5.8) overnight at 4°C, rinsed with 25 mM sodium acetate solution (pH 5.8), and stained with 0.05 vol/wt% cupromeronic blue solution for 3 h at 37 °C. Specimens were then rinsed with

25 mM NaOAc containing 0.1 M $MgCl_2$ and 2.5 vol% glutaraldehyde buffer for 30 min. Specimens were dehydrated in a series of solutions of ascending concentration of ethanol in water (25 to 90%) and then in absolute 100% ethanol and 100% propylene oxide. Specimens were infiltrated overnight in a 1:1 mixture of PO and LX-112 epoxy resin, and 2 h in 100% pure LX-112 resin. Sections of ~70 nm thickness (Leica Ultracut UCT model) were post-stained with 6% uranyl acetate and imaged (JEOL JEM-1220) at 80 kV.

2.6. Nano-dynamic mechanical properties

Nano-dynamic mechanical analysis was performed with biospecimens submersed in Hank's solution using a TI980 nano-indenter (Hysitron) and fluid cell Berkovich tip (n = 3). The static load was 800 μN and the dynamic load amplitude was 50 μN. Complex modulus (E*), storage modulus (E'), loss modulus (E"), and loss/damping factor (tan δ) were recorded as a function of frequency (10 Hz to 100 Hz). The storage modulus (E') represents the elastic energy stored in the sample, while the loss modulus (E") represents the viscous part of the energy lost by dissipation. The overall stiffness of the material subjected to a sinusoidal stress is measured by the complex modulus (E*). The loss/damping factor (tan δ, where δ is the phase angle between stress and strain) is the ratio of the E" over the E' and is a measure of how efficiently the material dissipates energy [47,48]. Measurements were obtained in eight different locations within each of two regions (cervical and apical). The impact of mineralized dentin, demineralization (organic matrix) and PG-depletion on the nanomechanical properties (E*, E', E" and tan δ) was calculated as absolute and relative (%) values. The absolute values were obtained by the variation of the moduli and tan δ of old and young dentin root region (cervical and apical). The relative values were calculated as a fold variation.

2.7. Statistical analysis

The study variables were age group (two levels: young and old), region (two levels: cervical and apical) and condition of dentin [three levels: mineralized, demineralized (organic matrix), and PG-depleted dentin]. The mean, standard deviation and error were calculated for all dependent variables. Data were analyzed with three-way, two-way and one-way ANOVA followed by Tukey or Games–Howell post hoc tests (SPSS v.25, SPSS). The level of significance was set at $\alpha = 0.05$.

3. Results

3.1. Characterization of dentin by Raman micro-spectroscopy (μ-Raman)

A group of indices from μ-Raman spectra were calculated to assess mineral and matrix composition (Fig 2A–B and Table S1). The mineral quality was assessed by two indices (MQ-1 and MQ-2). The MQ-1 index increased significantly with age, from 2.52 – 2.61 to 3.47 – 3.77, respectively in young and old dentin ($p = 0.003$), while there were no differences in MQ-2 index of young and old dentin ($p > 0.05$). Dentin mineralization was assessed using two mineral-to-matrix indices (MMR-1 and MMR-2). The mean of MMR-2 increased significantly with increasing age, with mean values of 3.14 – 3.73 and 4.72 – 5.28 for respectively young and old dentin ($p = 0.009$). There were no significant differences observed in MMR-1 index ($p = 0.067$).

Collagen post-translational modification (PTM), specifically enzymatic collagen cross-linking, and advanced glycation end-products (AGEs) were assessed using two indices (PTM-1 and PTM-2). Mean PTM-1 decreased with increasing age in cervical dentin from 1.52 in young to 1.01 in old dentin ($p = 0.018$). While in old dentin, PTM-1 was higher in apical (1.63) than in cervical (1.01) dentin ($p = 0.022$), there were no regional differences in young dentin ($p > 0.05$, Table S1). Although there were no significant differences in PTM-2 between young and old dentin, peak intensity at 1550 cm^{-1} in old dentin spectra (1.20 – 1.21) is significantly higher than in young (1.17 – 1.10), regardless of the region (Fig. 2A and Table S1).

Proteoglycan content and glycosaminoglycan chains (GAGs) sulfation pattern were assessed using the PG-1, PG-2 and SPGAG indices. PG-1, PG-2, and SPGAG were significantly lower in old dentin compared to young, with mean values decreasing from ~0.7 to 0.5 (PG-1), ~0.4 to 0.3 (PG-2) and ~0.6 to 0.4 (SPGAG), ($p = 0.044$, $p = 0.025$, and $p = 0.019$, respectively). The cervical region of old dentin (0.54) exhibited higher SPGAG values than apical (0.23) ($p = 0.014$), Table S1.

3.2. Ultrastructural and morphological features of type I collagen in young and old dentin

Fig. 3A–C shows the ultrastructural features obtained by SAXS of young and old cervical dentin, while different root dentin regions (cervical and apical) are depicted in Fig. S2 and S3A–C. The mean collagen *d*-spacing of mineralized, cervical dentin increased by $\Delta\bar{d} = 0.15$ nm with age ($p < 0.001$, Fig. 3A). Both the organic matrix (demineralized) and PG-depleted samples showed the opposite trend ($\Delta\bar{d} = -0.8$ *to* -1.2 nm, $p < 0.001$, Fig. 3A). While both age groups displayed a significant decrease in *d*-spacing following demineralization ($p < 0.001$), old dentin was affected to a greater extent (difference of means of 0.4 nm). PG depletion had no significant effect on *d*-spacing of old and young (cervical only) dentin, with a minimal mean difference of 0.02 and 0.06 nm, respectively ($p > 0.05$). However, there was a significant difference in *d*-spacing noted in the young apical region after PG depletion (difference of means of 0.27 nm, $p < 0.001$, Fig. S4A).

Mineralized dentin presented higher SAXS intensity values than the organic matrix and PG-depleted dentin, regardless of age ($p < 0.001$, Fig. 3B). There were no significant differences in intensity between young and old organic matrix ($p > 0.05$). However, in demineralized and PG-depleted dentin, there was a significant decrease in intensity ($p < 0.001$). Regional differences were present in young and old mineralized dentin, where higher intensity values were found in the apical than cervical region ($p < 0.001$), Fig. S3B.

Mineralized dentin presented a higher angular spread, and therefore lower degree of alignment, than the organic matrix and PG-depleted dentin, regardless of age ($p < 0.001$, Fig. 3C and S3C). Within both mineralized and organic matrix, but not PG-depleted dentin, the alignment decreased with increasing age ($p < 0.001$). Depletion of PGs decreased the alignment compared to young ($p < 0.001$) but not in the old organic matrix. PGs' removal increased the angular spread from 14.8° to 18.9° ($p < 0.001$) (Fig. 3C and S3C) in young dentin, while old dentin was not affected ($p > 0.05$).

Height maps obtained by atomic force microscopy revealed an intact and dense type I collagen fibril network in young dentin (Fig. 4A and S4A), while a modified collagen fibril network with areas of sparse interconnections in old dentin (Fig. 4B and S4C). Ultrastructural changes in young PG-depleted dentin were more apparent, with a distinct dissociation of collagen fibril bundles and the apparent unraveling of the collagen microfibrillar structure (Fig. 4C and S4B). Old PG-depleted dentin, on the other hand, presented a more compact distribution of collagen fibrils (Fig. 4D and S4D). The mean collagen fibril diameter (FD) varied from 160–178 nm and 166–204 nm in the organic matrix and PG-depleted dentin, respectively (Fig. 3D and S3D). The FD is significantly higher in old than in young dentin ($p = 0.012$). The removal of PGs led to a significant increase in the FD of young ($p < 0.001$) but not old dentin (Fig. 3D). There were no regional differences in FD (young/old, $p > 0.05$, Fig. S3D).

Transmission electron microscopy (TEM) analysis of the ultrastructure of the organic matrix of dentin revealed the presence collagen fibrils and stained GAGs (dark filaments) in young and old dentin (Fig. 4E–F and S5). Young dentin exhibited numerous densely packed collagen fibrils closely associated with GAGs. GAGs were particularly abundant in peritubular dentin (Fig. 4E and S5A–C). Conversely, old dentin presented irregular and less oriented collagen fibrils with a loosely packed network and apparent lower content of GAGs (Fig. 4F and S5D–F).

3.3. Nano-scale mechanical behavior of young and old dentin

Trends for complex, loss, and storage moduli were similar at a frequency of 20 Hz and load amplitude of 50 μN. For both cervical (Fig. 5A–C) and apical regions (Fig. S6A–C), moduli increased significantly with age, by a factor of 1.4–3, for mineralized dentin, the organic matrix (demineralized), and PG-depleted dentin ($p < 0.001$). Mineral removal reduced all moduli, regardless of region or age, by a factor of 3.7–5.3 ($p < 0.001$). Subsequent removal of PGs further reduced moduli, by ~1.6 GPa in young ($p < 0.001$), but not old cervical dentin. In general, moduli grouped by age and sample type (mineralized, organic matrix and PG-depleted dentin) were significantly higher for cervical than for apical dentin (Fig. S6A–C, $p < 0.001$). Exceptions are the loss modulus of young mineralized and the old organic matrix, where there was no significant difference between regions (Fig. S6B, $p > 0.05$).

Mineralized root dentin exhibits a small, but statistically significant increase in the damping factor ($\tan \delta$) with age (Fig. 5D and S6D, $p < 0.001$). The organic matrix exhibits a higher loss factor, which significantly degreases with age. This effect was much more pronounced in apical than in cervical dentin (Fig. S6D). Removal of PGs/GAGs had no significant effect in young dentin of either region but resulted in a small increase in loss factor for the old organic matrix (Fig. 5D); this effect was more pronounced in cervical than in the apical region (Fig. S6D). In general, the loss factor was higher in apical than in cervical dentin when samples were grouped by age and type (mineralized, organic matrix and PG-depleted dentin), $p < 0.05$.

4. Discussion

We present herein a comprehensive analysis of the impact of aging on the viscoelastic properties, composition and structural organization of human root dentin. A key feature of dentin is the ability to dissipate mechanical energy during mastication that would otherwise be available to generate microcracks and crack growth in enamel. In mid-coronal dentin, for instance, it has been shown that the loss modulus (E") decreases with age for frequencies greater than or equal to 10 Hz, while the storage modulus (E') is not affected [30]. As a consequence, the damping or loss factor (tan δ) – a measure of the fraction of the energy that is dissipated – decreases with age, consistent with age-related degradation of dentin strength, toughness, and resistance to fatigue [25–28,31,49]. Our results, however, show that root dentin has rather a different response to aging. Specifically, the complex (E*) and storage (E') moduli of native (mineralized) root dentin increase significantly with age, in both cervical and apical regions (Fig. 5 and S6). This means that the overall stiffness of root dentin increases. However, the relative increase of the loss modulus is greater than that of the storage (Table S2), and consequently the loss factor increases slightly in the apical (+1.6%) and more strongly in cervical dentin (+12.8%). The viscous response and ability to dissipate energy, therefore does not decrease with age. Root dentin appears to resist the effects of aging observed in other parts of the tooth, such as mid-coronal dentin [26,27,30].

We utilized μ-Raman spectroscopy to characterize the composition of the mineralized extracellular matrix (Fig. 2B and Table S1). Inspection of the impact of aging reveals that the mineral-to-matrix indices increase by 35% (MMR-1) to 45% (MMR-2). While the increase for MMR-2 is statistically significantly ($p = 0.009$), that of MMR-1 narrowly misses significance at the 95% level ($p = 0.067$). This could be due to a higher variance of the area of the amide I band compared to that of the CH_2 wagging band [43]. An increase in the degree of mineralization is expected based on the literature and is consistent with the increase in storage modulus and the increase in the diffracted intensity due to banded collagen fibrils observed in SAXS (Fig. 3B and S3B) and the greater decrease of the characteristic collagen *d*-spacing with demineralization in old dentin (Fig. 3A and S3A).

Interestingly, the average carbonate content increases with age (MQ-1), but the crystallinity is not affected (MQ-2), (Fig. 2B and Table S1). In parallel to these changes, we observed that the organic fraction experienced pronounced changes with age. The index of reducible collagen cross-linking decreases (PTM-1), while there were no significant changes in PTM-2. The increase in absolute peak intensity at ~1550 cm^{-1} in the spectra of old dentin (Fig. 2A), however, suggests an increase in the abundance of AGEs, consistent with age-related changes in post-translational modifications of other tissues [14,50–52]. Furthermore, there is strong evidence for a decrease in the PG abundance with age (PG-1 and −2 indices), also supported by the reduction in GAGs observed in TEM (Fig. 4E–F and S5) and by the reduction in the fraction of chondroitin sulfated in the 4-position (SPGAG); indicating that the chemical composition of PGs/GAGs is shifting as well. Thus, there is clear evidence that aging impacts the chemical composition of both the mineral and organic matrix of root dentin. Some of these trends provide plausible explanations for the changes in mechanical behavior. For instance, one would expect that an increase in the degree of mineralization with increasing age would increase the storage modulus of dentin. Similarly, an increase in

post-translational modifications such as AGEs is expected to stiffen the ECM as the collagen cross-linking density increases. However, both changes would be expected to reduce the loss factor rather than increase it. By nature, these experiments indicate correlation rather than causation. For deeper insights, we therefore deconstructed the dentin by first removing the mineral, and then depleting PGs and associated GAGs enzymatically. At each step we determined the dynamic mechanical properties and employed SAXS, AFM and TEM to obtain structural and compositional information.

Demineralization reduces moduli in young and old samples, on average by more than 70%, in both cervical and apical dentin (Fig. 5, S6 and Table S3). The effect is larger in old than in young dentin (Table S3). Moreover, while the characteristic collagen *d*-spacing of old mineralized dentin is slightly larger than that of young dentin (and closely matches data from mouse) [53], a greater decrease is shown upon demineralization (Fig. 3A and S3A). This change in the axial period by $\Delta d \sim -1$ nm is opposite in trend and smaller in magnitude ($\Delta d \sim +2–3$ nm) than what was observed in careful cryoTEM experiments, albeit of fixed periodontal ligament, cementum, and dentin [53–55]. Molecular dynamic simulations also indicate a significant shortening of collagen fibrils on mineralization of the gap zone [56], where it seems likely that the reason for the effect we observe, given that this is the first direct comparison of unfixed, hydrated, mineralized and demineralized human root dentin using the same technique, may be related to extrafibrillar rather than intrafibrillar mineral. Regardless of the mechanism, it appears that collagen fibrils in old root dentin not only shrink in the axial direction on demineralization but do so to a greater degree than young dentin. This may simply be a consequence of the larger degree of mineralization, but differences in the composition of the organic matrix cannot be ruled out at this time. While there is some information on the lateral spacing of collagen fibrils as a function of mineralization [57,58] there is only a small number of observations of the impact of demineralization on the axial *d*-spacing, and even less in the human dentin tissue.

The integrated intensity due to scattering from matter with the characteristic collagen *d*-spacing increases with age in mineralized dentin (Fig. 3B and S3B). Demineralization results in a greater attenuation of the intensity in old than in young samples. Overall, these results support the earlier prediction that old root dentin has a higher degree of mineralization. Thus, the impact of aging on dentin organic matrix is similar to that in the mineralized tissue, with one striking exception (Fig. 5, S6 and Table S4). While all moduli increase, the increase of the loss modulus is not sufficient to compensate for that of the storage modulus. Consequently, the loss factor of the dentin organic matrix and PG-depleted root dentin decreases sharply with increasing age in cervical (−31%) and apical (−47%) regions. The absolute and relative impact of aging is more pronounced in apical compared to cervical demineralized root dentin, Table S4.

The mechanical properties of the dentin organic matrix greatly depend on the hierarchical structure of collagen fibrils and the formation of inter-molecular collagen cross-links [11,33]. The spectroscopic analysis presented here demonstrates important modifications to the organic matrix, more specifically changes to collagen amide and AGE absorption bands (Fig. 2 and Table S1). Accumulation of AGEs has been suggested to increase collagen fibril stiffness and decrease interfibrillar slippage [59–61]. While we also find evidence for

collagen fragmentation (Fig. 4B–D, F and S4–5) that we expect to counteract the stiffening effect of AGEs, this effect seems to be less important, and the overall impact of aging is that the elastic response is favored over the viscous one. In this context, an interesting observation is that the angular spread of collagen is wider in old than in young dentin (Fig. 3C and S3C), indicating a decrease in order that may track with the increased degree of mineralization. Demineralization, however, decreases the angular spread (increases order) much less in old than in young dentin (Fig. 3C and S3C). A possible explanation for this result is that accumulation of AGEs in progressively more mineralized dentin reduces interfibrillar slippage and increase fibril stiffness [59–61], and thus limits the ability of the organic matrix to relax into a more ordered state on demineralization. Note that axial relaxation of collagen fibrils does not appear compromised in old dentin. While this provides a plausible explanation for the decrease in the loss factor of dentin organic matrix with age, the cause of this increase in loss modulus is not obvious.

Our findings clearly indicate that the abundance of PGs is reduced in old root dentin. PGs are known to bind significant amounts of water and impact the ECM viscosity [23]. As at least some damping in bone is supposed to arise from water movement in the pore space, PGs may play an important role in controlling dentin viscous response. Small leucine-rich PGs have a core protein and attached GAGs (Fig. 1A) that are highly sulfated complex polysaccharides [62,63]. PGs structurally contribute to the dentin framework by binding, stabilizing, and organizing collagen fibrils [64]. We therefore decided to probe whether the removal of PGs from dentin slabs impacts the mechanical properties of the organic matrix. Treatment of demineralized dentin slabs with matrix metalloprotease 3 (MMP-3) is an established method to deplete PGs, i.e. biglycan and decorin [35,36,65]. Certainly, for cervical young samples, but likely also in apical, PGs contribute to the overall stiffness of the ECM, and to both the elastic and viscous response. Based on the moderate increase of the loss factor that accompanies PG-depletion in cervical dentin (Fig. 5D), it appears that, at 20 Hz, PGs in the absence of mineral contribute less toward the dissipation of energy than expected. Interestingly, in old cervical dentin, the relative effect of PG-depletion on moduli is smaller than in young, consistent with the observation that the abundance of PGs decreases with age. Collectively, aging significantly impacts the dynamic mechanical properties of the dentin organic matrix and PG-depleted dentin (Table S5 and S6). Overall, the PG-depleted dentin stiffens, quite similarly to the dentin matrix with age. The storage modulus increases to a greater degree (Fig. 5 and S6), by a factor of 2–3, than the loss modulus (factor of 1.5–1.7). Consequently, the loss factor decreases with increasing age by 32% in cervical and 49% in apical samples (Table S6).

The enzymatic and non-enzymatic cross-linking patterns changed with age in the organic matrix (demineralized dentin). Old root dentin displays a collagen network that is axially more relaxed and with smaller *d*-spacing (Fig. 3A and S3A), but collagen fibrils are less aligned shown by greater azimuthal spread (Fig. 3C and S3C). Curiously, the collagen fibril diameter is reduced even though an axial relaxation would be expected to be present with an increase in diameter (Fig. 3D and 4C–D). The combination of these outcomes, with the reduction in integrated intensity (Fig. 3B), suggests that in old dentin, some collagen fibrils may have lost their characteristic periodicity and become amorphous. It remains somewhat perplexing that the dissipative behavior of mineralized old dentin does not follow the trend

of the demineralized tissue. This indicates that there is a mechanism to compensate for the loss of PGs and stiffening of the dentin matrix by AGE cross-linking, both of which we would expect to decrease the loss factor of the matrix with age. Notably, this mechanism seems to be active only in root, but not in mid-coronal dentin [26,27,30], and affect cervical root dentin more strongly than apical root dentin. By a process of elimination, we therefore hypothesize that changes in the interaction between matrix and mineral play an important role in the increase of loss factor and therefore the damping capacity of native old dentin. Given that there is no resorptive remodeling in dentin, we expect that the increased amount of carbonate present in older dentin (Fig. 2B and Table S1) is sequestered at surface of apatite crystals, where it has a disordering effect and may affect mineral-matrix bonding [66]. Additionally, the sulfation pattern of GAGs is reduced (SPGAG index, Fig. 2B and Table S1). These two effects may well be interdependent, as sulfation may affect the pH, and pH is an important factor for the incorporation of carbonate into apatite [67].

The depletion of PGs and changes in the sulfation pattern could differ between apical and cervical, and between root and coronal dentin, simply because root dentin may indirectly be affected by remodeling processes that occur in the close-by dental tissues such as the pulp and the periodontium. A weaker bond between the matrix and the mineral may help dissipate energy, thus increasing the loss factor despite the stiffening of the aging ECM. The decrease of PG abundance and the degree of sulfation of GAGs in older dentin point to a possible loss-of-function of the remaining PGs in the tissue, which may have a significant effect in tissue hydration and thereby compound changes in the viscoelastic behavior of the dentin tissue with age.

It is unclear whether these age-related modifications are merely a byproduct of physiological processes, or whether they are the result of a biological program in the aging tooth. Nonetheless, understanding the mechanisms by which root dentin escapes structural and functional modifications of aging may inspire strategies to halt or even reverse the process in coronal dentin or, more generally, other bone-type tissues.

5. Conclusions

A central finding is that the damping capacity (loss factor) of human root dentin does not degrade with age. Root dentin may therefore escape progressive embrittlement that is the hallmark of aging in coronal dentin and other bone-type mineralized tissues. This is even though biochemical alteration of prominent components of the organic matrix proceeds largely along the same lines as in other tissues, and results in the expected stiffening and loss of damping capacity. A plausible explanation for the discrepancy between the impact of aging on the organic matrix and that on the mineralized tissue comes from the observation that the carbonate content increases without impacting the crystallinity, indicating that it sequestered at the mineral surface. At the same time, the abundance of PGs decreases, and their sulfation patterns change, with likely changes in local pH and hydration. We therefore propose that a weakening mineral-matrix interface, possibly counterbalance the impact of collagen crosslinking maturity, accumulation of AGEs, and reduced content of PGs/GAGs.

Supplementary Material

Refer to Web version on PubMed Central for supplementary material.

Acknowledgements

The authors would like to thank Figen Seiler for processing and imaging at the Electron Microscopy Core facility of the University of Illinois at Chicago and Dr. Karen DeRocher (Northwestern University) participation in the small angle X-ray scattering (SAXS) data acquisition. This work was in part supported by the NIH (DE021040, DE025702, DE026952, GM103622). Use of the Pilatus 3 1M detector was provided by grant 1S10OD018090-01 (NIGMS). A portion of this work was performed at the Advanced Photon Source, a U.S. Department of Energy (DOE) Office of Science User Facility operated for the DOE Office of Science by Argonne National Laboratory under Contract No. DE-AC02-06CH11357.

REFERENCES

[1]. Harman D, The aging process, Proc. Natl. Acad. Sci. 78 (1981) 7124. 10.1073/pnas.78.11.7124. [PubMed: 6947277]

[2]. Phillip JM, Aifuwa I, Walston J, Wirtz D, The Mechanobiology of Aging, Annu. Rev. Biomed. Eng. 17 (2015) 113–141. 10.1146/annurev-bioeng-071114-040829. [PubMed: 26643020]

[3]. Hynes RO, Yamada KM, eds., Extracellular matrix biology, Cold Spring Harbor Laboratory Press, Cold Spring Harbor, N.Y, 2012.

[4]. Alliston T, Biological Regulation of Bone Quality, Curr. Osteoporos. Rep. 12 (2014) 366–375. 10.1007/s11914-014-0213-4. [PubMed: 24894149]

[5]. Frantz C, Stewart KM, Weaver VM, The extracellular matrix at a glance, J. Cell Sci. 123 (2010) 4195. 10.1242/jcs.023820. [PubMed: 21123617]

[6]. Haus JM, Carrithers JA, Trappe SW, Trappe TA, Collagen, cross-linking, and advanced glycation end products in aging human skeletal muscle, J. Appl. Physiol. 103 (2007) 2068–2076. 10.1152/japplphysiol.00670.2007. [PubMed: 17901242]

[7]. Akkus O, Adar F, Schaffler MB, Age-related changes in physicochemical properties of mineral crystals are related to impaired mechanical function of cortical bone, Bone. 34 (2004) 443–453. 10.1016/j.bone.2003.11.003. [PubMed: 15003792]

[8]. Boskey AL, Imbert L, Bone quality changes associated with aging and disease: a review: Bone quality changes, aging, and disease, Ann. N. Y. Acad. Sci. 1410 (2017) 93–106. 10.1111/nyas.13572. [PubMed: 29265417]

[9]. Burr DB, Changes in bone matrix properties with aging, Bone. 120 (2019) 85–93. 10.1016/j.bone.2018.10.010. [PubMed: 30315999]

[10]. Fedarko NS, Vetter UK, Weinstein S, Robey PG, Age-related changes in hyaluronan, proteoglycan, collagen, and osteonectin synthesis by human bone cells, J. Cell. Physiol. 151 (1992) 215–227. 10.1002/jcp.1041510202. [PubMed: 1572898]

[11]. Fratzl P, ed., Collagen: structure and mechanics, Springer, New York, 2008.

[12]. Paschalis EP, Verdelis K, Doty SB, Boskey AL, Mendelsohn R, Yamauchi M, Spectroscopic Characterization of Collagen Cross-Links in Bone, J. Bone Miner. Res. 16 (2001) 1821–1828. 10.1359/jbmr.2001.16.10.1821. [PubMed: 11585346]

[13]. Avery NC, Bailey AJ, The effects of the Maillard reaction on the physical properties and cell interactions of collagen, Pathol. Biol. (Paris). 54 (2006) 387–395. 10.1016/j.patbio.2006.07.005. [PubMed: 16962252]

[14]. Panwar P, Lamour G, Mackenzie NCW, Yang H, Ko F, Li H, Brömme D, Changes in Structural-Mechanical Properties and Degradability of Collagen during Aging-associated Modifications, J. Biol. Chem. 290 (2015) 23291–23306. 10.1074/jbc.M115.644310. [PubMed: 26224630]

[15]. Buckwalter JA, Kuettner KE, Thonar EJ-M, Age-related changes in articular cartilage proteoglycans: Electron microscopic studies, J. Orthop. Res. 3 (1985) 251–257. 10.1002/jor.1100030301. [PubMed: 4032100]

[16]. Boskey AL, Coleman R, Aging J Dent. Res. 89 (2010) 1333–1348. 10.1177/0022034510377791.

[17]. Li Y, Liu Y, Xia W, Lei D, Voorhees JJ, Fisher GJ, Age-dependent alterations of decorin glycosaminoglycans in human skin, Sci. Rep. 3 (2013) 2422. 10.1038/srep02422. [PubMed: 23939413]

[18]. Moronkeji K, Akhtar R, Mechanical Properties of Aging Human Skin, in: Derby B, Akhtar R (Eds.), Mech. Prop. Aging Soft Tissues, Springer International Publishing, Cham, 2015: pp. 237–263. 10.1007/978-3-319-03970-1_10.

[19]. Deschenes MR, Effects of Aging on Muscle Fibre Type and Size, Sports Med. 34 (2004) 809–824. 10.2165/00007256-200434120-00002. [PubMed: 15462613]

[20]. Vitályos G, Kolozsvári BL, Németh G, Losonczy G, Hassan Z, Pásztor D, Fodor M, Effects of aging on corneal parameters measured with Pentacam in healthy subjects, Sci. Rep 9 (2019) 3419. 10.1038/s41598-019-39234-x. [PubMed: 30833606]

[21]. Lin JB, Tsubota K, Apte RS, A glimpse at the aging eye, Npj Aging Mech. Dis. 2 (2016) 16003. 10.1038/npjamd.2016.3. [PubMed: 28721262]

[22]. Goldberg M, Dentin structure composition and mineralization, Front. Biosci E3 (2011) 711–735. 10.2741/e281.

[23]. Bertassoni LE, Dentin on the nanoscale: Hierarchical organization, mechanical behavior and bioinspired engineering, Dent. Mater. 33 (2017) 637–649. 10.1016/j.dental.2017.03.008. [PubMed: 28416222]

[24]. Li J, Parada C, Chai Y, Cellular and molecular mechanisms of tooth root development, Dev. Camb. Engl 144 (2017) 374–384. 10.1242/dev.137216.

[25]. Kinney JH, Nalla RK, Pople JA, Breunig TM, Ritchie RO, Age-related transparent root dentin: mineral concentration, crystallite size, and mechanical properties, Biomaterials. 26 (2005) 3363–3376. 10.1016/j.biomaterials.2004.09.004. [PubMed: 15603832]

[26]. Nazari A, Bajaj D, Zhang D, Romberg E, Arola D, Aging and the reduction in fracture toughness of human dentin, J. Mech. Behav. Biomed. Mater 2 (2009) 550–559. 10.1016/j.jmbbm.2009.01.008. [PubMed: 19627862]

[27]. Arola D, Reprogel RK, Effects of aging on the mechanical behavior of human dentin, Biomaterials. 26 (2005) 4051–4061. 10.1016/j.biomaterials.2004.10.029. [PubMed: 15626451]

[28]. Ivancik J, Majd H, Bajaj D, Romberg E, Arola D, Contributions of aging to the fatigue crack growth resistance of human dentin, Acta Biomater. 8 (2012) 2737–2746. 10.1016/j.actbio.2012.03.046. [PubMed: 22484693]

[29]. Yan W, Montoya C, Øilo M, Ossa A, Paranjpe A, Zhang H, Arola D, Reduction in Fracture Resistance of the Root with Aging, J. Endod 43 (2017) 1494–1498. 10.1016/j.joen.2017.04.020. [PubMed: 28712639]

[30]. Ryou H, Romberg E, Pashley DH, Tay FR, Arola D, Importance of age on the dynamic mechanical behavior of intertubular and peritubular dentin, J. Mech. Behav. Biomed. Mater 42 (2015) 229–242. 10.1016/j.jmbbm.2014.11.021. [PubMed: 25498296]

[31]. Bajaj D, Sundaram N, Nazari A, Arola D, Age, dehydration and fatigue crack growth in dentin, Biomaterials. 27 (2006) 2507–2517. 10.1016/j.biomaterials.2005.11.035. [PubMed: 16338002]

[32]. Ryou H, Romberg E, Pashley DH, Tay FR, Arola D, Nanoscopic dynamic mechanical properties of intertubular and peritubular dentin, J. Mech. Behav. Biomed. Mater. 7 (2012) 3–16. 10.1016/j.jmbbm.2011.08.010. [PubMed: 22340680]

[33]. Wallace JM, Chen Q, Fang M, Erickson B, Orr BG, Banaszak Holl MM, Type I Collagen Exists as a Distribution of Nanoscale Morphologies in Teeth, Bones, and Tendons, Langmuir. 26 (2010) 7349–7354. 10.1021/la100006a. [PubMed: 20121266]

[34]. Balooch M, Habelitz S, Kinney JH, Marshall SJ, Marshall GW, Mechanical properties of mineralized collagen fibrils as influenced by demineralization, J. Struct. Biol. 162 (2008) 404–410. 10.1016/j.jsb.2008.02.010. [PubMed: 18467127]

[35]. Boukpessi T, Menashi S, Camoin L, TenCate JM, Goldberg M, Chaussain-Miller C, The effect of stromelysin-1 (MMP-3) on non-collagenous extracellular matrix proteins of demineralized dentin and the adhesive properties of restorative resins, Biomaterials. 29 (2008) 4367–4373. 10.1016/j.biomaterials.2008.07.035. [PubMed: 18760468]

[36]. Alania Y, Creighton J, Trevelin LT, Zamperini CA, Bedran-Russo AK, Regional contribution of proteoglycans to the fracture toughness of the dentin extracellular matrix, J. Biomech. 101 (2020) 109633. 10.1016/j.jbiomech.2020.109633. [PubMed: 32035660]

[37]. Morris MD, Mandair GS, Raman Assessment of Bone Quality, Clin. Orthop. Relat. Res. 469 (2011) 2160–2169. 10.1007/s11999-010-1692-y. [PubMed: 21116756]

[38]. Khalid M, Bora T, Ghaithi AA, Thukral S, Dutta J, Raman Spectroscopy detects changes in Bone Mineral Quality and Collagen Cross-linkage in Staphylococcus Infected Human Bone, Sci. Rep 8 (2018) 9417. 10.1038/s41598-018-27752-z. [PubMed: 29925892]

[39]. Ellis R, Green E, Winlove CP, Structural Analysis of Glycosaminoglycans and Proteoglycans by Means of Raman Microspectrometry, Connect. Tissue Res. 50 (2009) 29–36. 10.1080/03008200802398422. [PubMed: 19212850]

[40]. Mainreck N, Brézillon S, Sockalingum GD, Maquart F-X, Manfait M, Wegrowski Y, Rapid Characterization of Glycosaminoglycans Using a Combined Approach by Infrared and Raman Microspectroscopies, J. Pharm. Sci. 100 (2011) 441–450. 10.1002/jps.22288. [PubMed: 20653053]

[41]. Ager JW, Nalla RK, Balooch G, Kim G, Pugach M, Habelitz S, Marshall GW, Kinney JH, Ritchie RO, On the Increasing Fragility of Human Teeth With Age: A Deep-UV Resonance Raman Study, J. Bone Miner. Res. 21 (2006) 1879–1887. 10.1359/jbmr.060816. [PubMed: 17002558]

[42]. Coyac BR, Falgayrac G, Penel G, Schmitt A, Schinke T, Linglart A, McKee MD, Chaussain C, Bardet C, Impaired mineral quality in dentin in X-linked hypophosphatemia, Connect. Tissue Res. 59 (2018) 91–96. 10.1080/03008207.2017.1417989. [PubMed: 29745817]

[43]. Unal M, Uppuganti S, Timur S, Mahadevan-Jansen A, Akkus O, Nyman JS, Assessing matrix quality by Raman spectroscopy helps predict fracture toughness of human cortical bone, Sci. Rep 9 (2019) 7195. 10.1038/s41598-019-43542-7. [PubMed: 31076574]

[44]. Jiratrakanvong J, Ma W, Agam G, Irving TC, MuscleX: a new tool for analyzing X-ray diffraction patterns from muscle and other fibrous systems, Acta Crystallogr. Sect. A. 74 (2018) a129. 10.1107/S0108767318098707.

[45]. Hammersley AP, Svensson SO, Thompson A, Calibration and correction of spatial distortions in 2D detector systems, Nucl. Instrum. Methods Phys. Res. Sect. Accel. Spectrometers Detect. Assoc. Equip 346 (1994) 312–321. 10.1016/0168-9002(94)90720-X.

[46]. Bedran-Russo AKB, Pereira PNR, Duarte WR, Okuyama K, Yamauchi M, Removal of dentin matrix proteoglycans by trypsin digestion and its effect on dentin bonding, J. Biomed. Mater. Res. B Appl. Biomater 85B (2008) 261–266. 10.1002/jbm.b.30944.

[47]. Menard KP, Dynamic mechanical analysis: a practical introduction, CRC Press, Boca Raton, FL, 2008.

[48]. Yamashita J, Li X, Furman BR, Rawls HR, Wang X, Agrawal CM, Collagen and bone viscoelasticity: A dynamic mechanical analysis, J. Biomed. Mater. Res. 63 (2002) 31–36. 10.1002/jbm.10086. [PubMed: 11787026]

[49]. Koester KJ, Ager JW, Ritchie RO, The effect of aging on crack-growth resistance and toughening mechanisms in human dentin, Biomaterials. 29 (2008) 1318–1328. 10.1016/j.biomaterials.2007.12.008. [PubMed: 18164757]

[50]. Marcos-Garcés V, Molina Aguilar P, Bea Serrano C, García Bustos V, Benavent Seguí J, Ferrández Izquierdo A, Ruiz-Saurí A, Age-related dermal collagen changes during development, maturation and ageing - a morphometric and comparative study, J. Anat. 225 (2014) 98–108. 10.1111/joa.12186. [PubMed: 24754576]

[51]. Bailey AJ, Paul RG, Knott L, Mechanisms of maturation and ageing of collagen, Mech. Ageing Dev. 106 (1998) 1–56. 10.1016/S0047-6374(98)00119-5. [PubMed: 9883973]

[52]. Knott L, Bailey AJ, Collagen cross-links in mineralizing tissues: A review of their chemistry, function, and clinical relevance, Bone. 22 (1998) 181–187. 10.1016/S8756-3282(97)00279-2. [PubMed: 9514209]

[53]. Quan BD, Sone ED, Structural changes in collagen fibrils across a mineralized interface revealed by cryo-TEM, Bone. 77 (2015) 42–49. 10.1016/j.bone.2015.04.020. [PubMed: 25892483]

[54]. Veis A, Collagen fibrillar structure in mineralized and nonmineralized tissues, Curr. Opin. Solid State Mater. Sci. 2 (1997) 370–378. 10.1016/S1359-0286(97)80130-1.

[55]. Beniash E, Traub W, Veis A, Weiner S, A Transmission Electron Microscope Study Using Vitrified Ice Sections of Predentin: Structural Changes in the Dentin Collagenous Matrix prior to Mineralization, J. Struct. Biol. 132 (2000) 212–225. 10.1006/jsbi.2000.4320. [PubMed: 11243890]

[56]. Depalle B, Qin Z, Shefelbine SJ, Buehler MJ, Large Deformation Mechanisms, Plasticity, and Failure of an Individual Collagen Fibril With Different Mineral Content, J. Bone Miner. Res. 31 (2016) 380–390. 10.1002/jbmr.2705. [PubMed: 26866939]

[57]. Bigi A, Ripamonti A, Koch MHJ, Roveri N, Calcified turkey leg tendon as structural model for bone mineralization, Int. J. Biol. Macromol. 10 (1988) 282–286. 10.1016/0141-8130(88)90005-0.

[58]. Bonar LC, Lees S, Mook HA, Neutron diffraction studies of collagen in fully mineralized bone, J. Mol. Biol. 181 (1985) 265–270. 10.1016/0022-2836(85)90090-7. [PubMed: 3981637]

[59]. Saito M, Marumo K, Collagen cross-links as a determinant of bone quality: a possible explanation for bone fragility in aging, osteoporosis, and diabetes mellitus, Osteoporos. Int 21 (2010) 195–214. 10.1007/s00198-009-1066-z. [PubMed: 19760059]

[60]. Tobe T, Shibata Y, Mochizuki A, Shimomura N, Zhou J, Wurihan R Tanaka S. Ikeda, Zhang Z, Li Q, Inoue T, Miyazaki T, Nanomechanical characterization of time-dependent deformation/recovery on human dentin caused by radiation-induced glycation, J. Mech. Behav. Biomed. Mater. 90 (2019) 248–255. 10.1016/j.jmbbm.2018.10.015. [PubMed: 30388508]

[61]. Kawamura M, Masaki C, Shibata Y, Kondo Y, Mukaibo T, Miyazaki T, Hosokawa R, Pentosidine correlates with nanomechanical properties of human jaw bone, J. Mech. Behav. Biomed. Mater 98 (2019) 20–25. 10.1016/j.jmbbm.2019.06.002. [PubMed: 31176091]

[62]. Prydz K, Determinants of Glycosaminoglycan (GAG) Structure, Biomolecules. 5 (2015) 2003–2022. 10.3390/biom5032003. [PubMed: 26308067]

[63]. Cheng H, Caterson B, Yamauchi M, Identification and Immunolocalization of Chondroitin Sulfate Proteoglycans in Tooth Cementum, Connect. Tissue Res. 40 (1999) 37–47. 10.3109/03008209909005276. [PubMed: 10770649]

[64]. Bertassoni LE, Swain MV, The contribution of proteoglycans to the mechanical behavior of mineralized tissues, J. Mech. Behav. Biomed. Mater. 38 (2014) 91–104. 10.1016/j.jmbbm.2014.06.008. [PubMed: 25043659]

[65]. Khaddam M, Salmon B, Le Denmat D, Tjaderhane L, Menashi S, Chaussain C, Rochefort GY, Boukpessi T, Grape seed extracts inhibit dentin matrix degradation by MMP-3, Front. Physiol 5 (2014). 10.3389/fphys.2014.00425.

[66]. Wopenka B, Pasteris JD, A mineralogical perspective on the apatite in bone, Mater. Sci. Eng. C. 25 (2005) 131–143. 10.1016/j.msec.2005.01.008.

[67]. Elliott JC, Calcium Phosphate Biominerals, Rev. Mineral. Geochem 48 (2002) 427–453. 10.2138/rmg.2002.48.11.

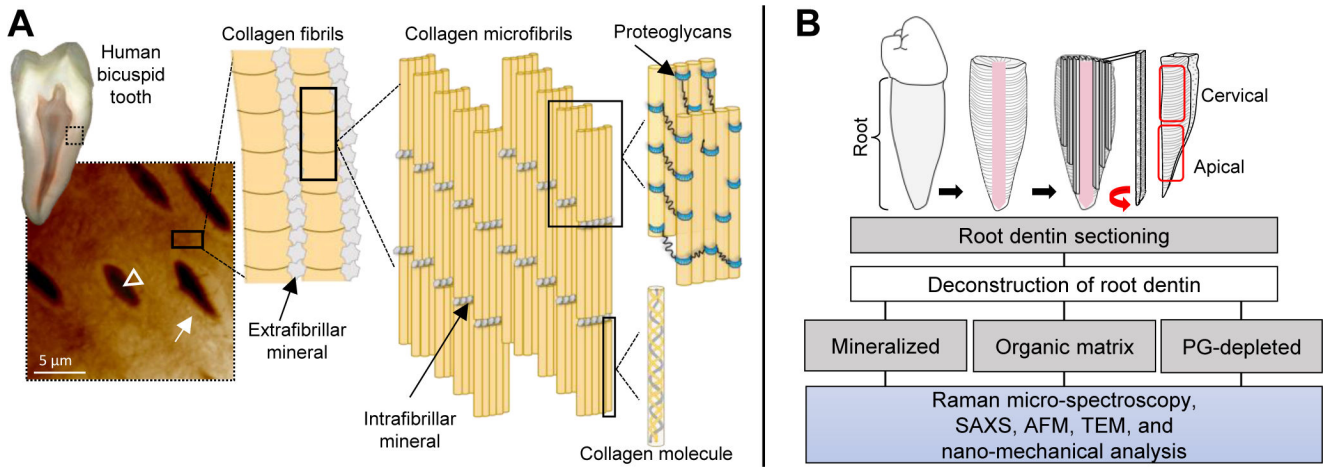

Fig. 1.

Structure of dentin of a human tooth and experimental pipeline of the analysis of root dentin. Cross-sectional view of a bicuspid tooth. Scanning probe microscopy image (20 × 20 µm) of root dentin with characteristic dentin tubules (arrowhead), highly mineralized peritubular dentin (closed arrows) surrounded by an extracellular matrix-rich intertubular dentin. Schematic depicts the main structural components of dentin, including extra-fibrillar and intra-fibrillar mineral, type I collagen fibrils and proteoglycans [core protein (blue) and glycosaminoglycan chains (black lines)]. Components are not up to scale (A). Workflow for preparation of samples of human bicuspid teeth. Mineralized, organic matrix (ECM) and PG-depleted samples from two age groups, young (18–25 y/o) and old (50–80 y/o) were compared and analyzed with Raman micro-spectroscopy, small angle X-ray scattering (SAXS), atomic force microscopy (AFM), transmission electron microscopy (TEM), and nano-dynamic mechanical analysis (B).

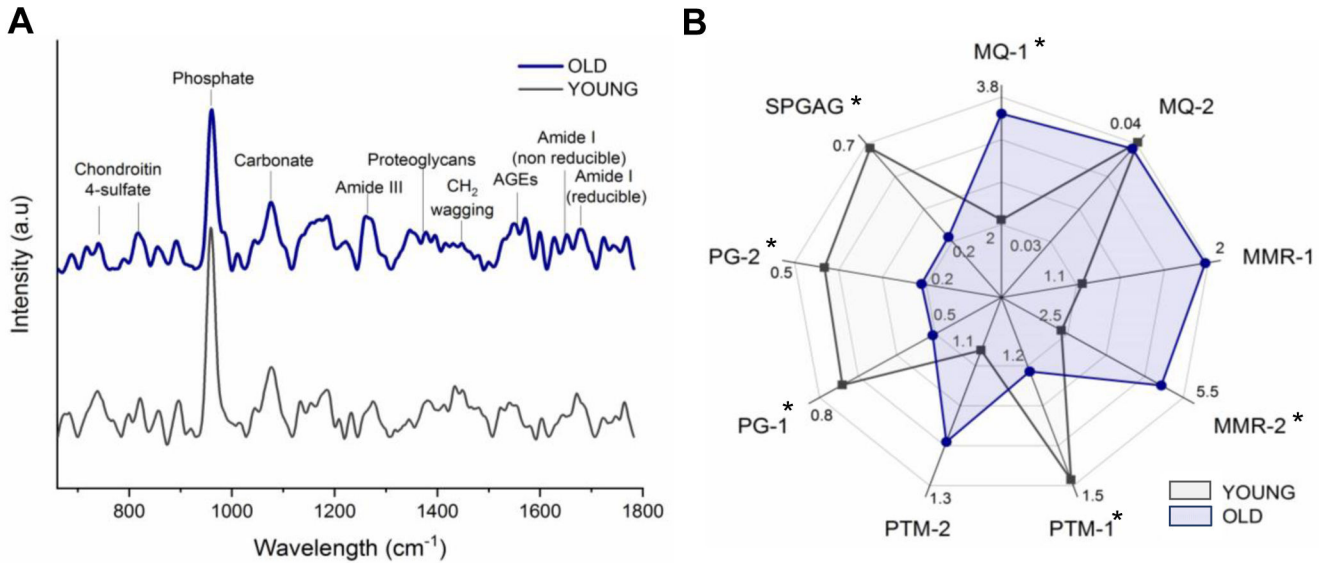

Fig. 2.

Chemical characterization of young and old dentin assessed by Raman micro-spectroscopy. Representative μ-Raman spectra of young (gray) and old dentin (dark blue) and the main bands used for calculation of investigated parameters (A). Radar chart depicts the mean values of analyzed indices (B), including mineral quality (MQ-1,2), mineral to matrix ratio (MMR1–2), collagen post-translational modification (PTM-1,2), proteoglycans (PG-1,2) and sulfation pattern of GAGs (SPGAG). Old dentin (dark blue) displays higher carbonation, MMRs, and PTM-2; but lower PTM-1, PGs, and sulfation pattern (SPGAG), than young dentin (gray), * $p < 0.05$. See Table S1 for associated bar plots.

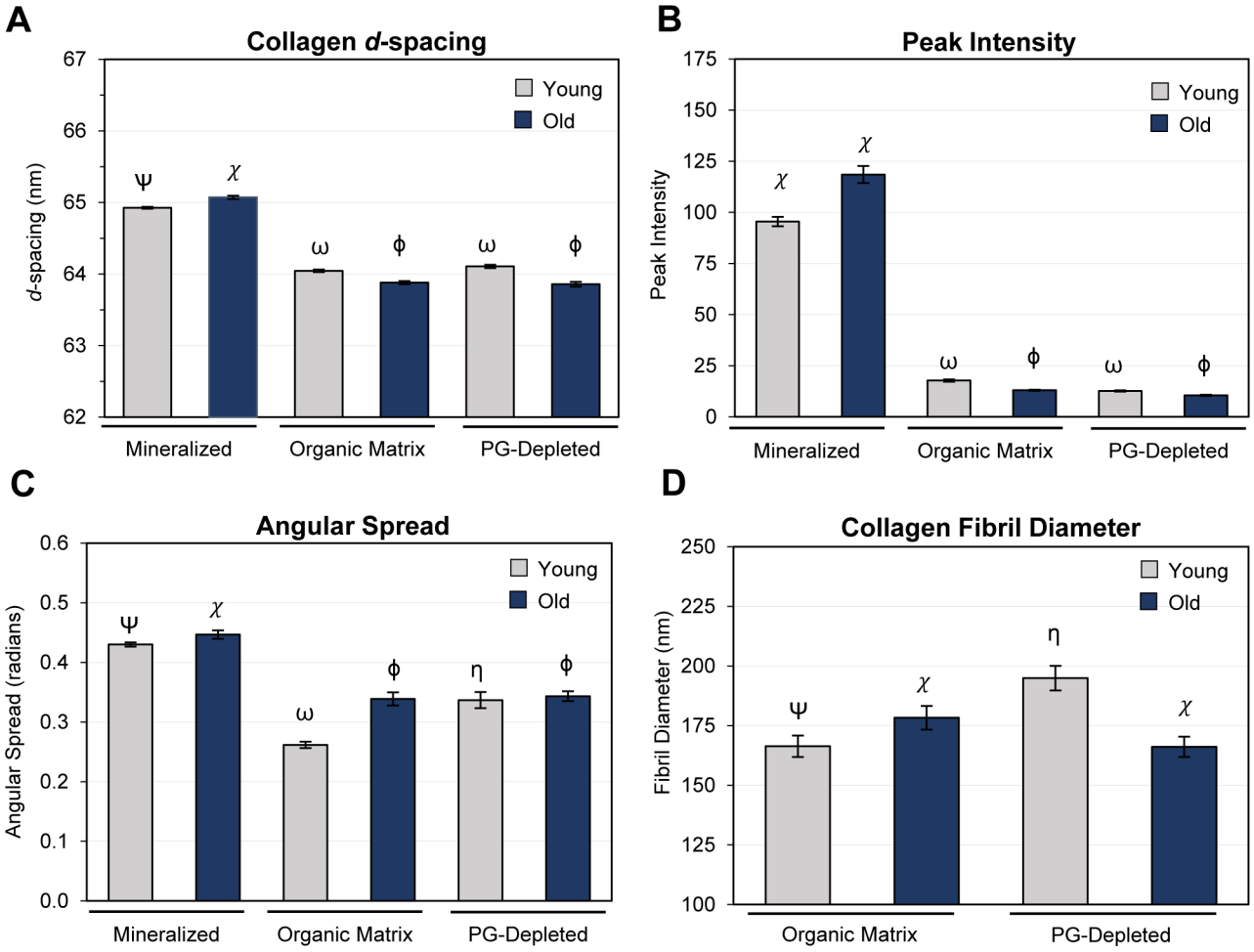

Fig. 3.

Impact of aging on collagen and biomineral in cervical root dentin as assessed by small-angle x-ray scattering (SAXS) and atomic force microscopy (AFM). Collagen periodicity (*d*-spacing, A), integrated collagen peak intensity (B), and azimuthal spread of collagen fibrils (C) were determined by 2D scanning SAXS performed on mineralized, demineralized (organic matrix), and PG-depleted dentin samples. Collagen fibril diameter (D) was determined from topographical maps of demineralized (organic matrix) and PG-depleted dentin acquired by AFM. Bar graphs depict the mean and the standard error of the mean for each group. Groups labeled with different Greek letters have statistically significant differences of means within the age groups ($p < 0.05$). For comparison of cervical and apical regions, see Supplemental Information Fig. S3.

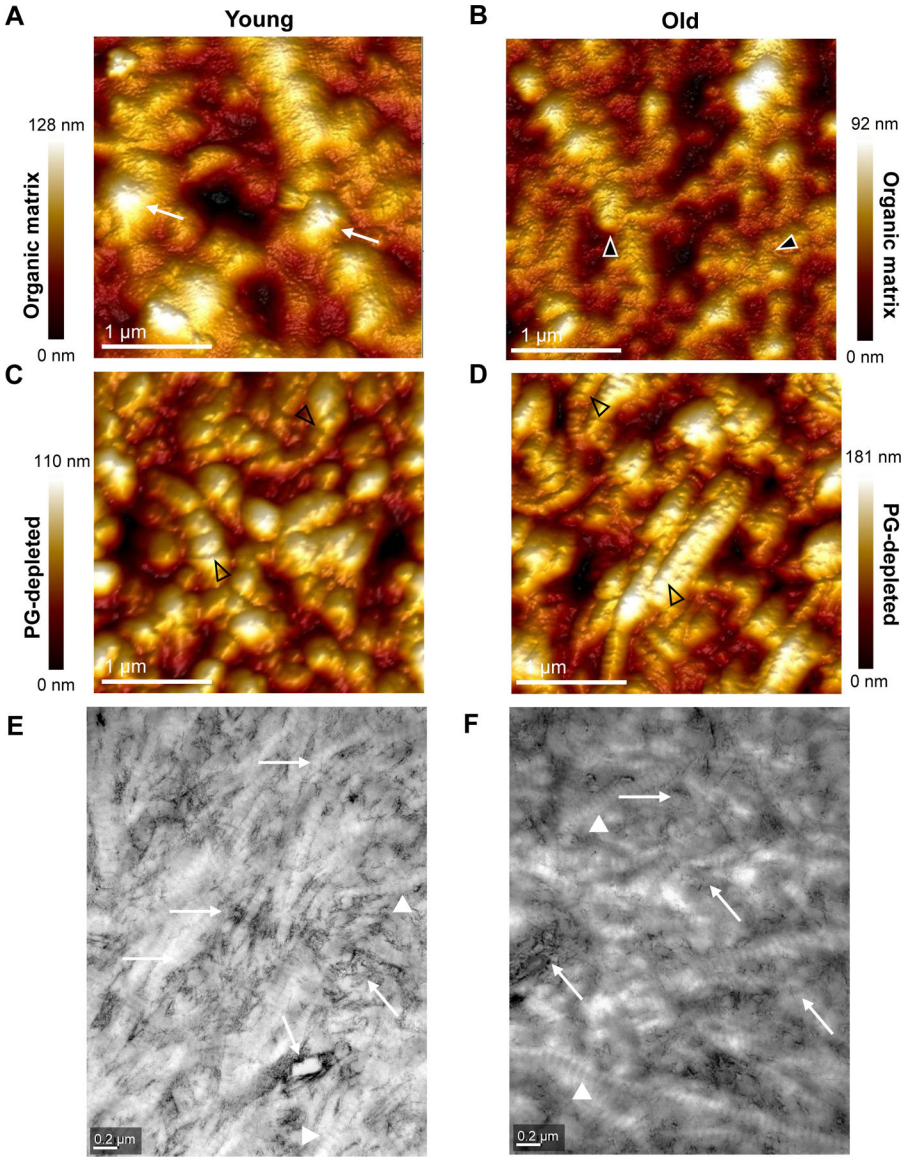

Fig. 4.

Ultrastructure of dentin extracellular matrix assessed by atomic force microscopy (AFM) and transmission electron microscopy (TEM). AFM height maps of young (A, C) and old (B, D) apical root dentin organic matrix (A, B) and PG-depleted dentin (C, D). Note long and relatively smooth fibrils on the surface of young samples (A, white arrows) and a more irregular appearance in old dentin (B, arrowheads). In PG-depleted samples, the banding pattern of collagen fibrils with a characteristic periodicity (~67 nm) is more apparent (C, D, arrowheads). TEM images with bright-field contrast of thin sections of young (E) and old (F) cervical root dentin organic matrix, depicts typical banding pattern of collagen fibrils, more evident in young dentin. There is an apparent decrease of the amount in PGs-associated glycosaminoglycan chains (dark filaments) around dentinal tubules and particularly the intratubular dentin (white arrows) of old dentin when compared to young.

For additional AFM height maps see Supplementary Information Fig. S4, and for additional TEM images see Fig. S5.

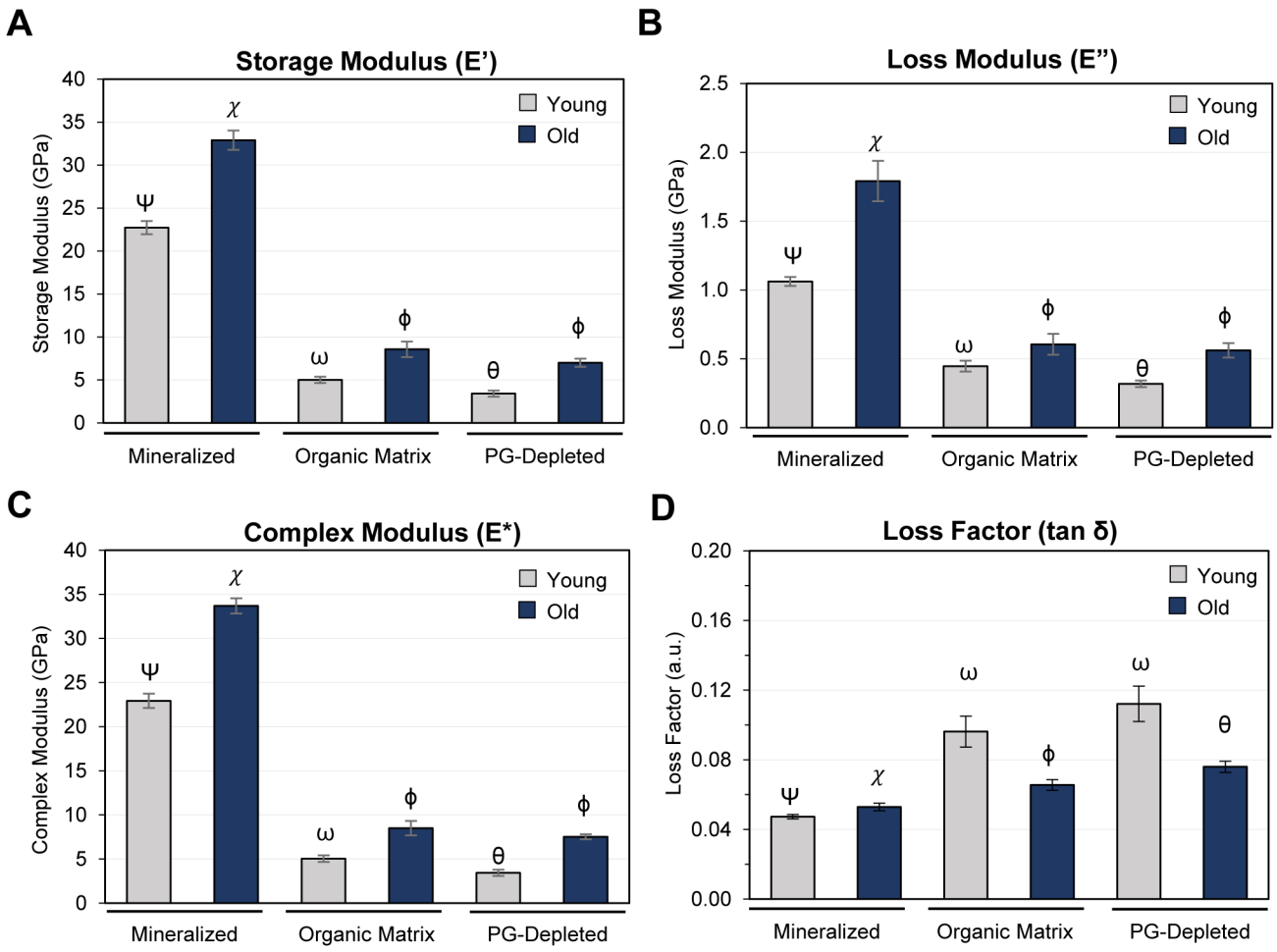

Fig. 5.

Nano-scale viscoelastic properties of cervical root dentin assessed by dynamic mechanical analysis (DMA). Bar graphs depict the storage (A), loss (B), complex (C) moduli, and loss or damping factor (tan δ, D) determined by nano-dynamic mechanical analysis performed on mineralized, demineralized (organic matrix), and PG-depleted dentin samples at a frequency of 20 Hz and load amplitude of 50 μN. Bar graphs depict the mean and the standard error of the mean for each group. Groups labeled with different Greek letters have statistically significant differences of means within the age groups and dentin ($p < 0.05$). Comparison of cervical and apical regions in Supplementary Information Fig. S6 and Tables S2–6.